

# Role of Molecular Entanglements in Starch Fiber Formation by Electrospinning

Lingyan Kong – Pennsylvania State University

Gregory R. Ziegler – Pennsylvania State  
University

Deposited 05/19/2020

Citation of published version:

Kong, L., Ziegler, G. (2012): Role of Molecular Entanglements in Starch Fiber Formation by Electrospinning. *Biomacromolecules*, 13(8).

DOI: <https://doi.org/10.1021/bm300396j>

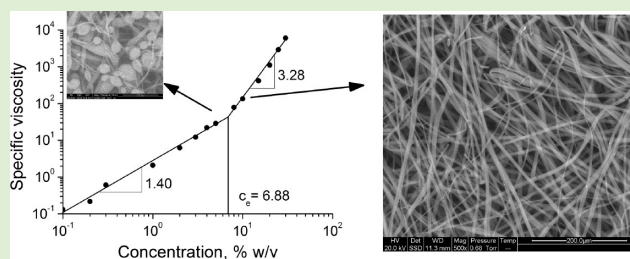
# Role of Molecular Entanglements in Starch Fiber Formation by Electrospinning

Lingyan Kong and Gregory R. Ziegler\*

Department of Food Science, Pennsylvania State University, 341 Food Science Building, University Park, Pennsylvania, United States

## Supporting Information

**ABSTRACT:** We have demonstrated a method of fabricating pure starch fibers with an average diameter in the order of micrometers. In the present study, correlation between the rheological properties of starch dispersions and the electrospinnability was attempted via the extrapolation of the critical entanglement concentration, which is the boundary between the semidilute unentangled regime and the semidilute entangled regime. Dispersions of high amylose starch containing nominally 80% amylose (Gelose 80) required 1.2–2.7 times the entanglement concentration for effective electrospinning. Besides starch concentration, molecular conformation, and shear viscosity were also of importance in determining the electrospinnability. The rheological properties and electrospinnability of different starches were studied. Hylon VII and Hylon V starches, containing nominally 70 and 50% amylose, respectively, required concentrations of 1.9 and 3.7 times their entanglement concentrations for electrospinning. Only poor fibers were obtained from mung bean starch, which contains about 35% amylose, while starches with even lower amylose contents could not be electrospun.



## INTRODUCTION

Electrospinning is a technology of growing interest for producing submicrometer or nanoscale fibers.<sup>1</sup> Among methods of achieving fibers of this diameter, electrospinning is a peerless technique in terms of its cost-effectiveness, simplicity, general applicability, and controllability of fiber properties. Similar to the development of conventional fiber spinning technology, most efforts have been directed toward electrospinning of synthetic polymer systems. Yet there is a growing need for better utilization of biopolymers and development of synthetic biofibers. In addition to a sustainable and renewable supply of their constituent biopolymers, biofibers have advantages pertaining to their inherent biodegradability and biocompatibility. Therefore, a variety of biopolymers, including polysaccharides, proteins, and DNA, have been successfully spun into fibers, especially by electrospinning.<sup>2</sup>

Starch is among the most abundant and inexpensive biopolymers. Starch is found in plant tissues, such as leaves, stems, seeds, roots, and tubers. It is also found in certain algae and bacteria. Starch exists in semicrystalline granules of different size, shape and morphology depending on its botanical source. Nevertheless, most starches are composed of two structurally distinct molecules: amylose, a linear or lightly branched (1→4)-linked  $\alpha$ -glucopyranose, and amylopectin, a highly branched molecule of (1→4)-linked  $\alpha$ -glucopyranose with  $\alpha$ -(1→6) branch linkages. The amylose/amylopectin ratio in starches also varies with botanical origin.

Many attempts to spin starch fibers have been reported in both the academic and patent literature. The fabrication of

starch-containing fibers has been dependent upon the addition of nonstarch components, for example, other polymers, plasticizers, or cross-linkers. Electrospinning has been utilized to spin other polymers, for instance, polycaprolactone,<sup>3</sup> poly(vinyl alcohol),<sup>4</sup> polylactic acid,<sup>5</sup> and poly(lactide-co-glycolide) with added starch.<sup>6</sup> However, the addition of starch was detrimental to the electrospinnability of the polymer mixture in most cases, so it is reasonable to suggest that starch behaved more as a filler to replace a limited portion of the polymer in the fiber, rather than serving as the principal fiber-forming material.

We have recently demonstrated that pure starch fibers can be produced by electrospinning.<sup>7</sup> The method is based on the selection of an appropriate solvent, which is able to dissolve starch to establish sufficient chain entanglements for fiber spinning. Amylose helices have been shown to adopt a random coil conformation in a certain range of dimethyl sulfoxide (DMSO) concentration.<sup>8</sup> DMSO or DMSO/water mixtures would thus be a good candidate solvent; starch molecules are fully extended in certain DMSO solvent systems and entanglement could easily be established. Therefore, we hypothesized that if entanglement of starch molecules is a determinant factor for the starch to be electrospun, then starch concentrations exceeding the entanglement concentration would be required for effective spinning.

Received: March 14, 2012

Revised: June 1, 2012

Published: June 18, 2012

A number of researchers have tried to establish the correlation between polymer chain entanglements and the ability to electrospin. McKee et al.<sup>9</sup> suggested that the polymer concentration must be at least 2–2.5 times the entanglement concentration to electrospin fibers. The entanglement concentration,  $c_e$ , is defined as the boundary between the semidilute unentangled regime and the semidilute entangled regime of a polymer solution. In the semidilute unentangled regime, polymer chains overlap one another but do not entangle, whereas in the semidilute entangled regime, polymer chains significantly overlap one another such that individual chain motion is constrained.

Among biopolymers, the rheological properties of chitosan in 80% aqueous acetic acid solution has been studied<sup>10</sup> and the critical entanglement concentration was found to be 2.9% (w/w). However, the researchers were unable to fabricate chitosan fibers at any concentration. The authors hypothesized that even though the chitosan molecules might well entangle at concentrations above 2.9%, the high viscosity of these highly deacetylated chitosan solutions constrained electrospinning. This suggests that entanglement alone is perhaps necessary but insufficient for electrospinning.

Rheological properties of the spinning dope play a crucial role in determining the fiber forming ability of the polymer dispersion. In the current study, we attempted to investigate how solution viscosities of starch in DMSO/water mixtures impacted their electrospinnability. We hypothesized that the starch concentration must exceed the entanglement concentration for fiber formation. Starches of different amylose content were studied to gain understanding of the generalizability of the correlation between rheological properties and electrospinnability.

## EXPERIMENTAL SECTION

**Materials.** Gelose 80 starch was kindly provided by Penford Food Ingredients Company (Centennial, CO) and used as received. Gelose 80 is a corn starch with amylose content of about 80%. Hylon VII, Hylon V, Melojel, and Amioca starches were supplied by National Starch and Chemical Company (now Corn Products International, Bridgewater, NJ). They are all corn starches with amylose content according to the manufacturer of approximately 70, 55, 25, and 0–1%, respectively. Mung bean starch was purified from a mung bean starch powder product from a local Asian market. The mung bean starch powder was dispersed in deionized water and allowed to precipitate. The precipitate was washed with 50% (v/v) ethanol in water for 3 times and finally with pure ethanol and dried. Mung bean starch has an amylose content of about 35%, according to the literature.<sup>11</sup> Ethanol (200 proof) and dimethyl sulfoxide (DMSO) were obtained from VWR International (Radnor, PA).

**Electrospinning.** The preparation of spinning dope involved dissolving the appropriate amount of starch in an aqueous DMSO solution. The starch dispersion was heated in a boiling water bath with continuous stirring on a magnetic stirrer hot plate for about one hour. The starch dispersion was then allowed to cool to room temperature and deaerated. A 10 mL syringe (Becton, Dickinson and Company, Franklin Lakes, NJ) with a 20 gauge blunt needle was used as the spinneret.

The electrospinning setup comprised a high voltage generator (ES40P, Gamma High Voltage Research, Inc., Ormond Beach, FL), a syringe pump (81620, Hamilton Company, Reno, NV), and a grounded metal mesh immersed in pure ethanol (Figure 1). This electrospinning configuration can also be referred to as “electro-wet-spinning”. The fibrous mat deposited in the ethanol coagulation bath was then washed using pure ethanol and dried in a desiccator containing Drierite under vacuum. Electrospinning was conducted at room temperature ( $\approx 20$  °C) in this study.

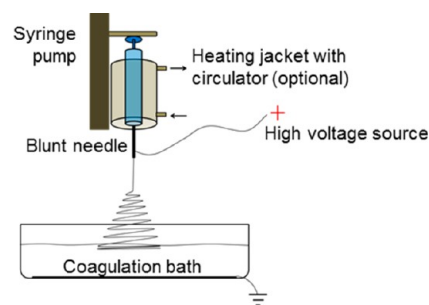


Figure 1. Schematic drawing of the electrospinning setup.

The electrospinnability was not evaluated under constant process parameters. Instead, the electrospinnability of each starch dispersion was evaluated while varying three spinning parameters (feed rate, voltage, and spinning distance) within predetermined ranges: feed rates of 0.1, 0.25, and 0.4 mL/h, and spinning distances of 5, 7.5, and 10 cm. At each feed rate and spinning distance combination, the voltage was gradually increased from 0 to 15 kV. The onset and ending voltages of continuous jet formation were recorded. The electrospinnability for starch dispersions was determined by visual and microscopic observation of the fibers formed.

**Rheology.** Starch dispersions in aqueous DMSO solutions were prepared for rheological characterization. DMSO concentration ranged from 70 to 100% (v/v). For each DMSO concentration, starch concentrations of 0.1 to 30% (w/v) were prepared. Flow curves, that is, shear viscosity versus shear rate, were generated using cone and plate geometry on a strain-controlled rheometer (ARES, TA Instrument, New Castle, DE). The cone and plate diameters were 50 mm and the gap was set at 0.043 mm. The cone angle was 0.04 radians. Viscosity data were collected in the shear rate range from 0.1 to 100  $s^{-1}$  at 20 °C.

**Characterization.** Fiber morphology was examined using an Olympus BX41 optical microscope (Hitech Instruments, Edgemont, PA) equipped with cross polarizers and a SPOT Insight QE camera (SPOT Diagnostic Instruments, Sterling Heights, MI). Image analysis was completed using SPOT analytical and controlling software. Observation of fibers was also performed using a FEI Quanta 200 ESEM (FEI, Hillsboro, OR) in low vacuum mode at an accelerating voltage of 20 keV.

## RESULTS AND DISCUSSION

**Rheological Properties.** Flow curves of Gelose 80 starch in pure DMSO with varying starch concentrations are given in Figure 2. Unreliable data, that is, out of the detection limit of the rheometer, were not plotted. Pure DMSO and dispersions

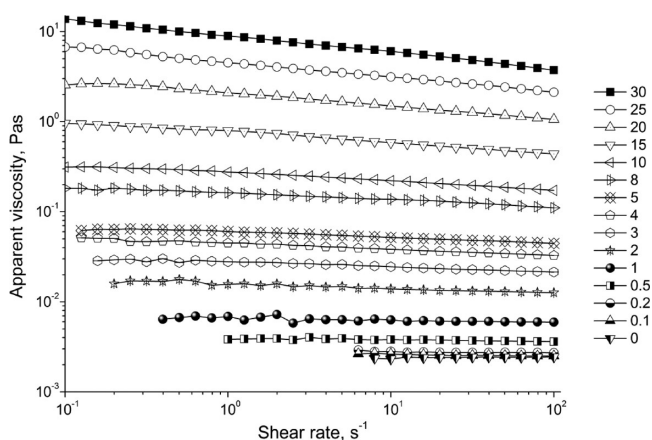
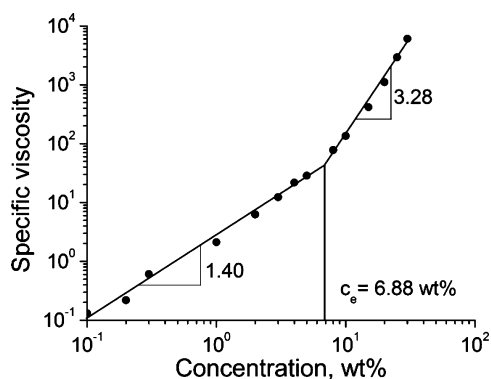


Figure 2. Flow curves of Gelose 80 starch in 100% DMSO as a function of starch concentration (% w/v) at 20 °C.

of low starch concentrations approached Newtonian behavior, that is, shear viscosity was independent of shear rate; up to 10% (w/v) of starch, the dispersions did not show significant shear thinning. As starch concentration was increased beyond 10% (w/v) shear thinning became apparent. By fitting the power law model,  $\eta = K\dot{\gamma}^{n-1}$ , to the data for 30% (w/v) Gelose 80 starch dispersions, the power law index,  $n$ , was calculated to be 0.82, indicating the presence of a weak shear thinning effect; the viscosity decreased less than 1 order of magnitude over three decades of shear rate.

Zero shear viscosities,  $\eta_0$ , were approximated from the flow curves by using the actual or extrapolated values for apparent viscosity at  $0.1 \text{ s}^{-1}$ , and used to calculate specific viscosity,  $\eta_{sp} = (\eta_0 - \eta_s)/\eta_s$ . To determine the entanglement concentration,  $c_e$ , specific viscosity data were plotted against starch concentration. The  $c_e$  was, thus, determined to be 6.88% (w/v) from the intercept of the fitted slopes in the semidilute unentangled and the semidilute entangled regimes (Figure 3). In the semidilute



**Figure 3.** Plot of specific viscosity versus Gelose 80 starch concentration in 100% DMSO. The entanglement concentration and slopes of fitted lines in two regimes are illustrated.

unentangled regime, the specific viscosity,  $\eta_{sp}$ , was proportional to  $c^{1.40}$ . This concentration dependence is close to reported values for chitosan in 80% aqueous acetic acid solution ( $\eta_{sp} \sim c^{1.3}$ ),<sup>10</sup> and for linear and branched poly(ethylene terephthalate-co-ethylene isophthalate) (PET-co-PEI) in mixture solvent chloroform/dimethylformamide ( $\eta_{sp} \sim c^{1.41}$ ) and ( $\eta_{sp} \sim c^{1.39}$ ), respectively.<sup>9</sup> This scaling dependence is also close to the theoretically predicted value ( $\eta_{sp} \sim c^{1.25}$ ) for neutral, linear polymers in semidilute unentangled regime in a good solvent.<sup>12</sup>

In the semidilute entangled regime, we observed that  $\eta_{sp} \sim c^{3.28}$ , lower than theoretical prediction ( $\eta_{sp} \sim c^{4.8}$ )<sup>12</sup> and some reported values ( $\eta_{sp} \sim c^{6.0}$ ) for linear PET-co-PEI<sup>10</sup> and chitosan.<sup>9</sup> However, this concentration dependence is very close to that of other random coil polysaccharides, that is, 3.3.<sup>13</sup> The small exponent suggests that the starch molecules were entangled but did not interact strongly. The presence of branched amylopectin (about 20%) could also contribute to the weak dependence of specific viscosity on concentration. McKee et al.<sup>9</sup> reported a scaling dependence ( $\eta_{sp} \sim c^{2.73}$ ) for branched PET-co-PEI in the semidilute entangled regime, lower than that for linear PET-co-PEI, ( $\eta_{sp} \sim c^{6.0}$ ).

The flow curves of Gelose 80 in a series of DMSO solutions from 100 to 70% were also obtained and can be found in the Supporting Information. The general trend from low to high starch concentration is similar to starch in pure DMSO. However, the starch dispersions of intermediate concentrations (3–10% w/w) developed complicated flow behavior in DMSO

lower than 90%. The shear viscosity increased with shear rate and decreased after a peak viscosity. DMSO aqueous solutions lower than 90% might be insufficient to completely dissociate starch molecules.

Entanglement concentration values for starch in different DMSO solutions were obtained by plotting specific viscosity versus starch concentration (Figure 4). Exponents of the concentration dependence in the unentangled regime ranged from 1.20 to 1.80, indicating weak interaction of individual molecules and absence of significant entanglements. Exponents of the concentration dependence in the entangled regime ranged from 2.66 to 3.03 for DMSO concentration greater than 85%. The dependence becomes stronger for starch in 75 and 70% aqueous DMSO solutions. These DMSO solutions were not able to totally dissolve the starch, which significantly increased the starch dispersion viscosity. This was evidenced from visual observation of the dispersion; starch in 75 and 70% DMSO solutions appeared as an opaque white suspension, in contrast to the transparent or translucent yellowish dispersion of starch in more concentrated DMSO solutions. This transition occurred at about 85% DMSO making measurement of the viscosities at this concentration highly unstable and preventing an accurate determination of  $c_e$ .

The entanglement concentration  $c_e$  is plotted with respect to DMSO concentration in Figure 5. In the range of 100–90% DMSO where starch can be effectively dissolved, the entanglement concentration  $c_e$  reaches a minimum at 2.14% (w/v) in 92.5% DMSO, suggesting that solvation is highest at 92.5% aqueous DMSO. With better solvation extended coils occupy a larger hydrodynamic volume so that the overlap concentration is lower.

**Correlation with Electrospinnability.** A series of starch dispersions in each DMSO concentration was subject to electrospinning on the apparatus shown in Figure 1. The fiber forming ability (electrospinnability) was examined in the predetermined process parameter ranges. A spinnability map illustrating regions of spinnability at varying concentrations of DMSO and starch was constructed (Figure 6). Starch dispersions with good fiber forming ability are marked in the shaded area. During the spinning of these dispersions, a continuous and stable jet could be induced and fibers were deposited on the surface of the ethanol bath without accompanying sprayed particles. Optical microscopy and scanning electron microscopy were also employed to evaluate the fiber morphology. Good fibers are continuous, uniform, smooth, and defect-free (Figure 7b–j). At lower concentrations, electrospinning was constantly interrupted by electro-spraying using parameters outside of the shaded area and producing mixtures of poor and short fibers and particles. Poor fibers are too fragile to be collected from the coagulation bath. Microscopic observation of the poor fibers shows lack of uniformity, defects and presence of debris (Figure 7a). Electrospinning also occurred at high concentrations outside the shaded area at low feed rates. In addition, at high feed rates the jet did not develop whipping instability and the process appeared like simple wet-spinning.

If we consider the concentration at which good fibers start to form as the critical concentration for electrospinnability  $c^*$ ,  $c^*/c_e$  values can be obtained for Gelose 80 starch in different DMSO concentrations. These values are 1.7, 2.7, 1.2, and 2.3 for Gelose 80 starch in 100, 95, 90, and 80% DMSO aqueous solutions, respectively. Our findings agree well with previous reported  $c^*/c_e$  values<sup>9,14</sup> for electrospinning defect-free fibers.

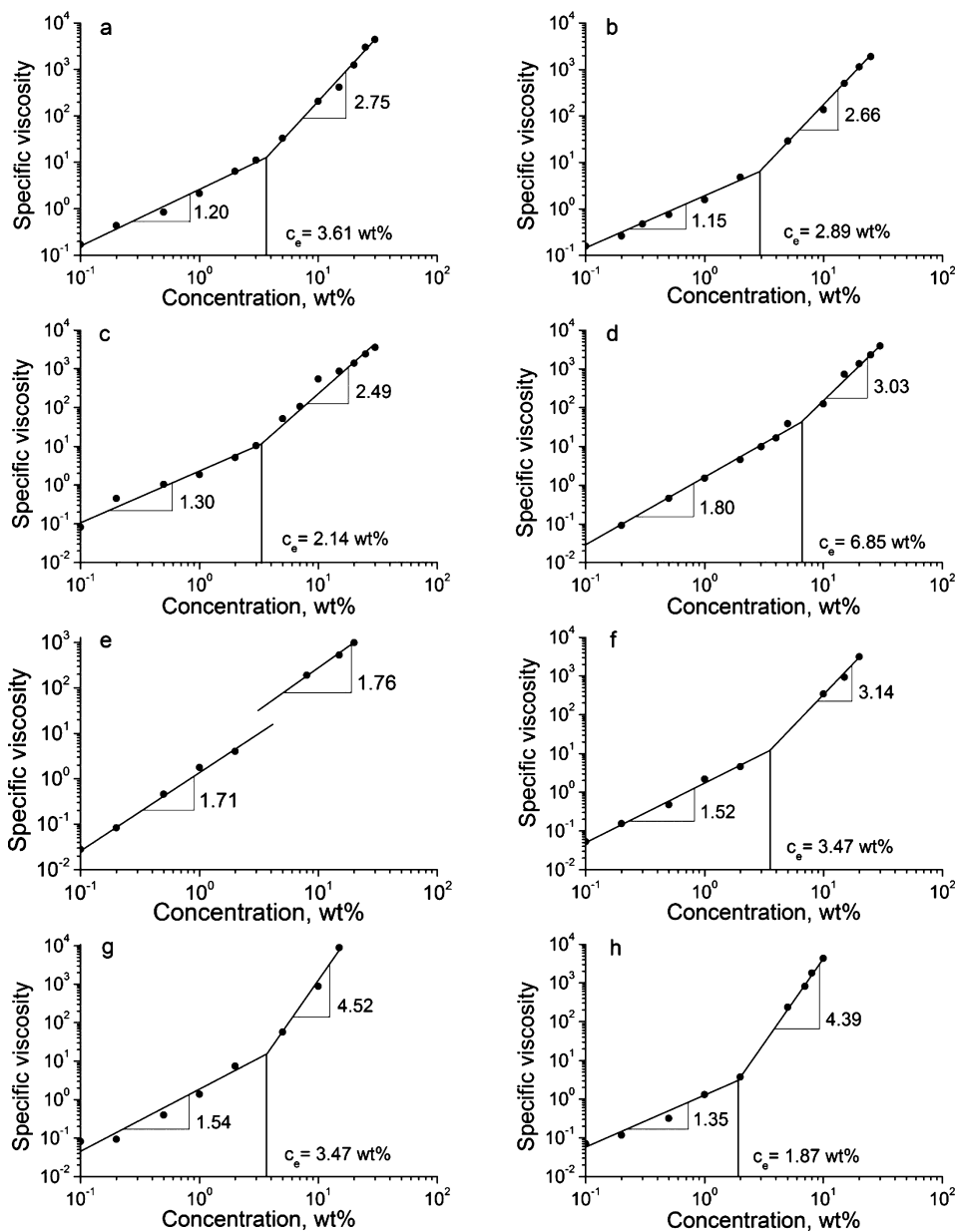


Figure 4. Plots of specific viscosity versus Gelose 80 starch concentration in (a) 97.5, (b) 95, (c) 92.5, (d) 90, (e) 85, (f) 80, (g) 75, and (h) 70% (v/v) DMSO aqueous solutions. The entanglement concentrations and slopes of fitted lines in two regimes are illustrated.

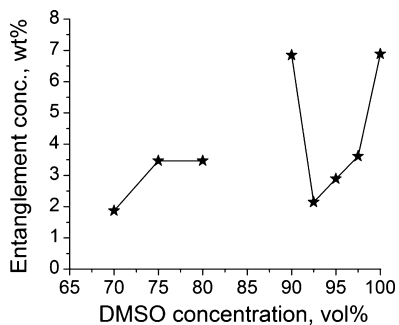


Figure 5. The entanglement concentrations of Gelose 80 starch as a function of DMSO concentration.

Other factors may also influence the electrospinnability of a starch–DMSO–water dispersion, for example, Klossner et al.,<sup>10</sup> were unsuccessful electrospinning chitosan in 80% acetic acid at

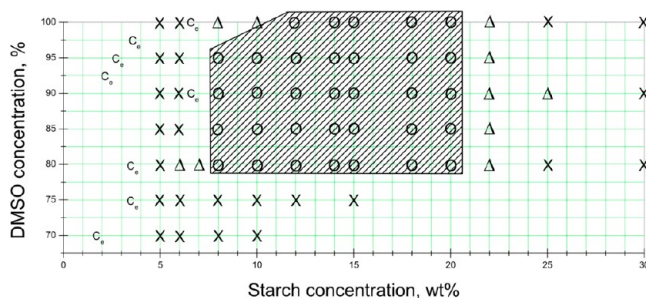
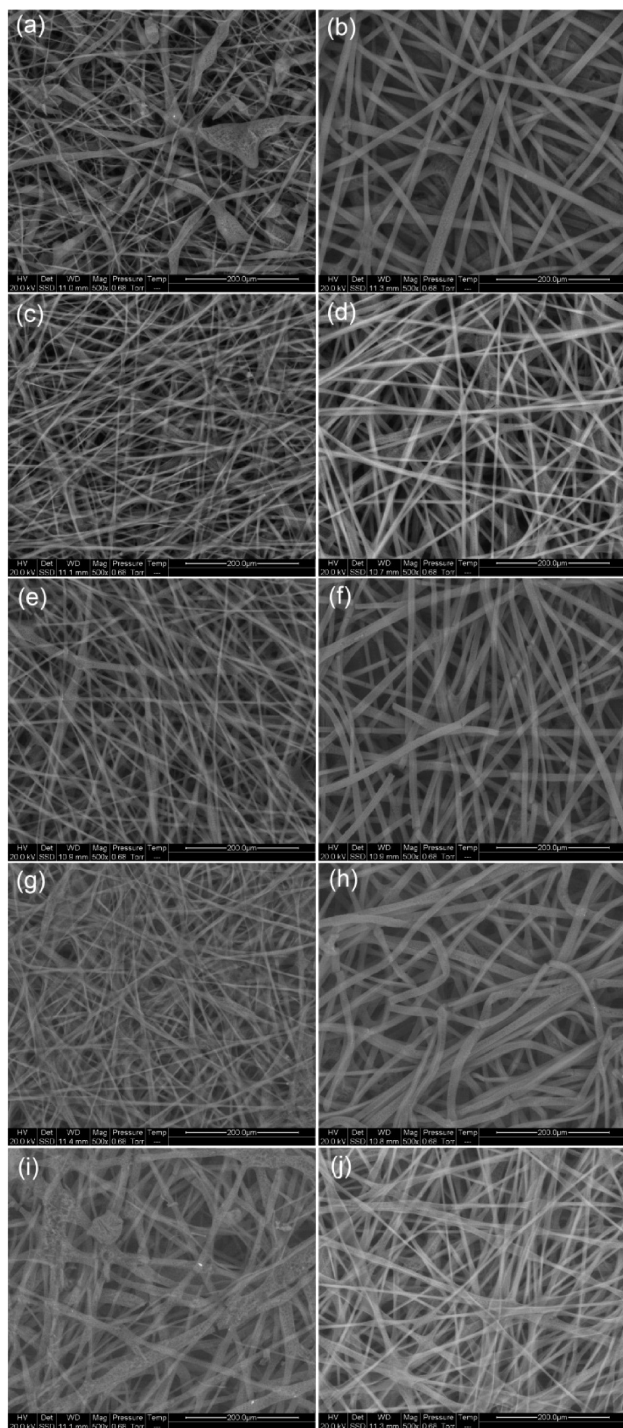
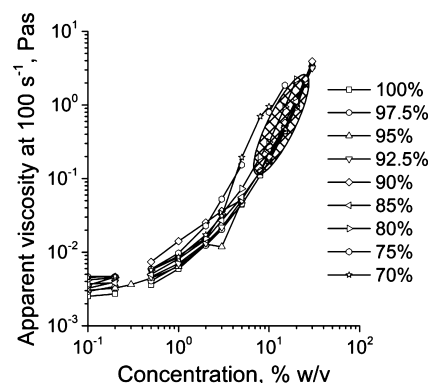


Figure 6. Evaluation of fiber formation abilities from starch dispersions of different starch and DMSO concentration: good fiber formed (circles), poor fiber formed (triangles), and no fiber formed (Xs). Shaded area represents the electrospinnable region. Entanglement concentrations are also approximately labeled.



**Figure 7.** Scanning electron micrographs of electrospun pure gelose 80 starch fibers from (a) 8% and (b) 12% (w/v) starch in 100% DMSO, (c) 8% and (d) 10% (w/v) starch in 95% DMSO, (e) 8% and (f) 10% (w/v) starch in 90% DMSO, (g) 8% and (h) 10% (w/v) starch in 85% DMSO, and (i) 8% and (j) 10% (w/v) starch in 80% DMSO. Scale bar represents 200  $\mu\text{m}$  in all figures.

concentrations 2–2.5 times  $c_e$ , which they attributed to the high viscosity (4–16 Pa·s). Therefore, the shear viscosities at  $100 \text{ s}^{-1}$  were plotted against starch concentrations and the region of spinnability denoted (Figure 8). From this graph, one can observe that all the electrospinnable dispersions have a shear viscosity clustered in the shade area, that is, from 0.2 to 2.2 Pa·s. At higher concentrations, where sufficient molecular entangle-



**Figure 8.** Shear viscosities (at  $100 \text{ s}^{-1}$ ) of the Gelose 80 starch dispersions as a function of starch concentration in different DMSO concentrations. All electrospinnable dispersions fall into the shade area.

ment has been well established, the high viscosity of the Gelose 80 starch dispersion could be the factor that limits electrospinnability. At lower concentrations in the range from  $c_e$  to  $c^*$ , where molecular entanglement was also fulfilled, the low viscosity and absence of shear thinning suggested that the entanglement of the starch molecules was insufficient. While the shear viscosity at  $100 \text{ s}^{-1}$  is here correlated with electrospinnability, it should be noted that the actual shear rate involved in electrospinning must be much higher than  $100 \text{ s}^{-1}$ .<sup>15</sup> It is so far concluded that starch conformation, presence of entanglement and shear viscosity together influence the electrospinnability of a starch–DMSO–water dispersion.

As aforementioned, the electrospinnability was not evaluated under constant process parameters. If the parameters had been set constant, the electrospinnable window would have been smaller than the current shaded area. In the experiment, starch dispersions from the left edge of the shaded area were found to be inappropriate for electrospinning at a low feeding rate, large spinning distance and low voltage. The situation was reversed for concentrated starch dispersions. For example, an 8% (w/v) starch dispersion in 80% DMSO was only spinnable at the highest feeding rate and the shortest spinning distance in this study. A continuous jet and fibers began to form when the voltage was increased to 10 kV, but the jet became unstable when the voltage reached 12 kV. In another example, good fibers from 20% (w/v) starch in 100% DMSO were only obtainable at the largest spinning distance and lowest feeding rate. At a spinning distance of 10 cm and voltage of 10 kV, increasing the feed rate from 1 to 2 mL/h resulted in good fibers becoming poor fibers.

These phenomena are related to the rheological properties of the starch dispersions. From the flow curves, highly concentrated starch dispersions (e.g., 20% (w/v)) develop shear thinning at lower shear rates than moderately concentrated starch dispersions (e.g., 8–10%, w/v). Hence, higher feeding rate and higher voltage/spinning distance (i.e., higher shear rate) are required to develop sufficient molecular alignment and shear thinning for moderately concentrated starch dispersions. On the contrary, highly concentrated starch dispersions do not require such high shear rate for orienting the starch molecules in the flow. The spinning parameters, including starch concentration, thus interact. The parameter combinations appropriate for electrospinning are roughly illustrated in Figure 9. Further research is required to study

the interaction of electrospinning parameters through sound design of experiment.

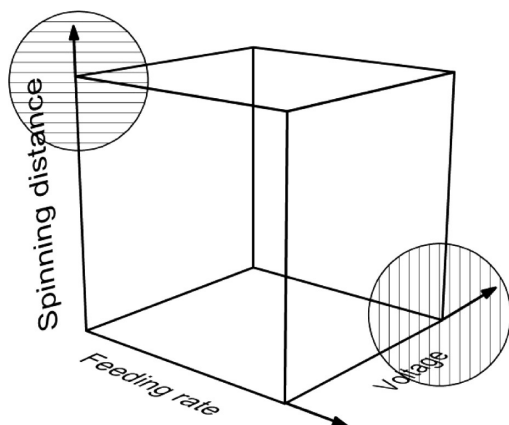


**Figure 9.** Three-dimensional coordinates of spinning parameters. Shaded circles estimate the appropriate parameter combinations for electrospinning starch dispersion from highly concentrated (horizontal lines) and moderately concentrated (vertical lines) dispersions.

**Effect of Amylose/Amylopectin Ratios.** Starches of different amylose/amylopectin ratios in 95% aqueous DMSO were characterized by rheological measurements. Flow curves can be found in the supporting material. By plotting specific viscosities versus starch concentrations, the entanglement concentration  $c_e$  values were obtained (Figure 10a–e). The

exponents of the concentration dependence in the semidilute unentangled and entangled regimes are all in good agreement with that of Gelose 80 starch. Weak entanglements were formed in the semidilute entangled regime, which became weaker as amylopectin content increases. This is expected since amylose is the major contributor to extended coils and their entanglements, though larger, amylopectin behaves as a hard ellipsoid. The entanglement concentration  $c_e$  is the highest in Hylon VII starch (4.15%, w/v) and decreases to 0.29% (w/v) for Mejojel starch, probably due to the high molecular weight of amylopectin. A  $c_e$  value was not obtainable within the concentration range of this experiment for waxy maize starch that has 0–1% amylose content. The exponents of concentration dependence in the entangled regime were found to be consecutively decreasing as amylose content decreased. In high amylose starches, where amylose entanglements dominate, the molecules interpenetrate into one another and can be well entangled. As the amylose content decreases, the amylose molecules contribute less and the amylopectin components dominate, and these bulky objects cannot entangle much.

The electrospinnability of starches of different amylose content were evaluated (Figure 11). Electrospinning of Hylon VII starch in 95% DMSO was successful in the concentration range of 8–20% (w/v). This range becomes smaller and smaller as amylose content in the starch decreases. The electrospinnable range for Hylon V shrinks to between 10 and 15% (w/v). Poor mung bean starch fibers were only obtainable from a concentration around 7% (w/v). Melojel and Amioca starches were not electrospinnable at any concentration in 95%

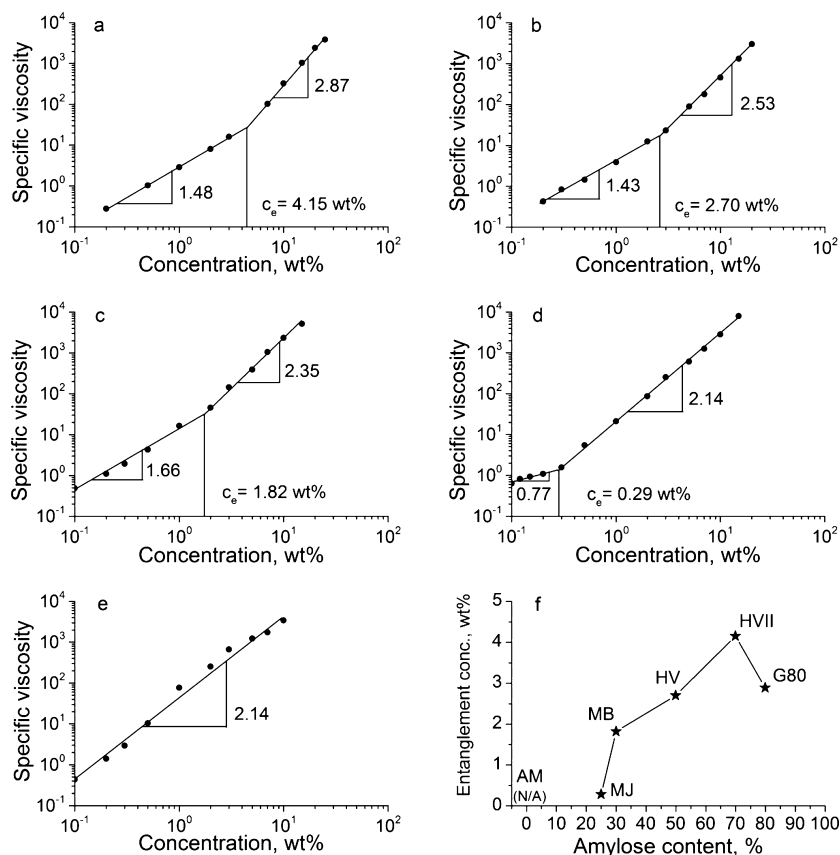


**Figure 10.** Plots of specific viscosity versus starch concentration for (a) Hylon VII (HVII), (b) Hylon V (HV), (c) Mung bean starch (MB), (d) Mejojel starch (MJ), and (e) Amioca waxy maize starch (AM) in 95% (v/v) DMSO aqueous solution and plot of entanglement concentration as a function of amylose content in the starches.

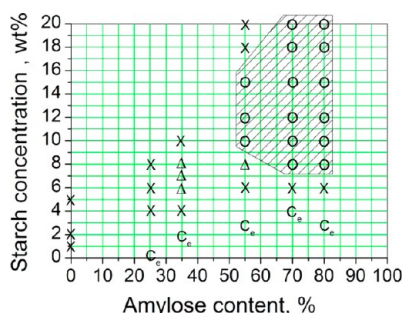


**Figure 11.** Evaluation of electrospinnability from starch dispersions of different starches in 95% DMSO: good fiber formed (circles), poor fiber formed (triangles), and no fiber formed (Xs). The starches have varying amylose content: Amioca (0–1%), Melogel (25%), mung bean starch (30%), Hylon V (55%), and Hylon VII (70%). Shaded area represents the electrospinnable region. Entanglement concentrations are also approximately labeled.

DMSO. Electron micrograph figures of electrospun fibers show this trend (Figure 12).

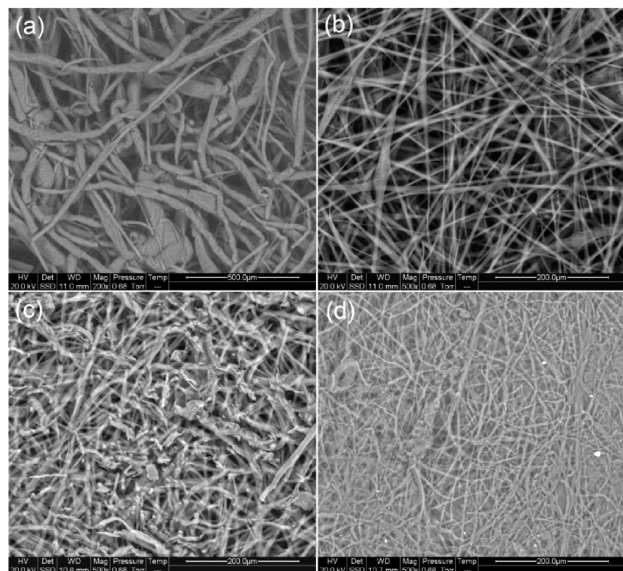


**Figure 12.** Scanning electron micrographs of electrospun pure starch fibers from (a) 18% (w/v) Hylon V, (b) 8% (w/v) Hylon VII, (c) 8% (w/v) Hylon V, and (d) 7% (w/v) Mung bean starch in 95% (v/v) DMSO aqueous solutions. Scale bar represents 200  $\mu\text{m}$  in all figures.

The  $c^*/c_e$  values were determined to be 3.8, 3.7, and 1.9 for mung bean starch, Hylon V, and Hylon VII, respectively. The  $c^*/c_e$  value of Hylon VII is the only one falls into the previous reported range. The Hylon V and mung bean starch need a higher concentration to be electrospun, probably due to their lower content of amylose, though molecular weight and other characteristics may also be of importance in the establishment of chain entanglement.

## CONCLUSIONS

In conclusion, rheological properties and the correlation with electrospinnability of Gelose 80 starch in different DMSO solutions were studied. To obtain well-formed fibers, the concentration of starch had to be 1.2–2.7 times the entanglement concentration  $c_e$ , depending on the DMSO concentration. In addition to the establishment of molecular

entanglements, molecular conformation, and shear viscosity are also of importance in determining the electrospinnability.

## ASSOCIATED CONTENT

### Supporting Information

Flow curves of Gelose 80 starch in 97.5, 95, 92.5, 90, 85, 80, 75, and 70% (v/v) DMSO as a function of starch concentration at 20 °C. Flow curves of Hylon VII starch, Hylon V starch, Mung bean starch, Melogel starch, and Amioca starch in 95% (v/v) DMSO as a function of starch concentration at 20 °C. This material is available free of charge via the Internet at <http://pubs.acs.org>.

## AUTHOR INFORMATION

### Corresponding Author

\*Tel.: +1-814-863-2960. Fax: +1-814-863-6132. E-mail: [grzl@psu.edu](mailto:grzl@psu.edu)

### Notes

The authors declare no competing financial interest.

## ACKNOWLEDGMENTS

This work is funded by the USDA National Institute for Food and Agriculture, National Competitive Grants Program, National Research Initiative Program 71.1 FY 2007 as Grant No. 2007-35503-18392.

## REFERENCES

- (1) Ramakrishna, S.; Fujihara, K.; Teo, W.-E.; Lim, T.-C.; Ma, Z. *An Introduction to Electrospinning and Nanofibers*; World Scientific: River Edge, NJ, 2005.
- (2) Kong, L.; Ziegler, G. R.; Bhosale, R., Fibers spun from polysaccharides. In *Handbook of carbohydrate polymers: development, properties, and applications*; Ito, R.; Matsuo, Y., Eds.; Nova Science Pub Inc.: New York, 2010; pp 1–43.
- (3) Jukola, H.; Nikkola, L.; Gomes, M. E.; Reis, R. L.; Ashammakhi, N. *AIP Conf. Proc.* **2008**, *973*, 971–974.
- (4) Suckyte, J.; Adomaviciute, E.; Milasius, R. *Fibres Text. East. Eur.* **2010**, *18*, 24–27.
- (5) Sunthornvarabhas, J.; Chatakanonda, P.; Piyachomkwan, K.; Sriroth, K. *Mater. Lett.* **2011**, *65*, 985–987.
- (6) Zhang, G.; Xu, J. *Adv. Mater. Res.* **2010**, *160–162*, 1062–1066.
- (7) Kong, L.; Ziegler, G. R. *Carbohydr. Polym.* **2012**, Submitted.
- (8) De Vasconcelos, C. L.; Pereira, M. R.; Fonseca, J. L. C. *J. Appl. Polym. Sci.* **2001**, *80*, 1285–1290.
- (9) McKee, M. G.; Wilkes, G. L.; Colby, R. H.; Long, T. E. *Macromolecules* **2004**, *37*, 1760–1767.
- (10) Klossner, R. R.; Queen, H. A.; Coughlin, A. J.; Krause, W. E. *Biomacromolecules* **2008**, *9*, 2947–2953.
- (11) Hoover, R.; Li, Y. X.; Hynes, G.; Senanayake, N. *Food Hydrocolloids* **1997**, *11*, 401–408.
- (12) de Gennes, P. G. *Scaling Concepts in Polymer Physics*; Cornell University Press: Ithaca, NY, 1979.
- (13) Morris, E. R.; Cutler, A. N.; Ross-Murphy, S. B.; Rees, D. A.; Price, J. *Carbohydr. Polym.* **1981**, *1*, 5–21.
- (14) Chen, H.; Elabd, Y. A. *Macromolecules* **2009**, *42*, 3368–3373.
- (15) Greiner, A.; Wendorff, J. H. Functional self-assembled nanofibers by electrospinning. In *Self-Assembled Nanomaterials I*; Shimizu, T., Ed.; Springer: New York, 2008; pp 107–171.